arXiv:1606.02095v1 [cond-mat.soft] 7 Jun 2016

Mechanism of chain collapse of strongly charged polyelectrolytes

Anvy Moly Tom,[1,*] Satyavani Vemparala,[1,†] R. Rajesh,[1,‡] and Nikolai V. Brilliantov[2,§]

[1] *The Institute of Mathematical Sciences, C.I.T. Campus, Taramani, Chennai 600113, India*
[2] *Department of Mathematics, University of Leicester, Leicester LE1 7RH, United Kingdom*

(Dated: June 8, 2016)

We perform extensive molecular dynamics simulations of a charged polymer in a good solvent in the regime where the chain is collapsed. We analyze the dependence of the gyration radius R_g on the reduced Bjerrum length ℓ_B and find two different regimes. In the first one, called as a weak electrostatic regime, $R_g \sim \ell_B^{-1/2}$, which is consistent only with the predictions of the counterion-fluctuation theory. In the second one, called a strong electrostatic regime, we find $R_g \sim \ell_B^{-1/5}$. To explain the novel regime we modify the counterion-fluctuation theory.

PACS numbers: 82.35.Rs, 82.37.Np, 61.25.he

Introduction. The conformational states of a flexible neutral polymer in different solvents are well known. It is extended in a good solvent due to favorable excluded volume interactions with the solvent molecules and collapses into a compact globule in a bad solvent [1–3]. In contrast, a flexible polyelectrolyte (PE) – charged polymer in the presence of counterions – undergoes an extended to collapsed transition in both good and bad solvents. Unlike neutral polymers, the conformations of a PE depend not only on the solvent quality, but also crucially on the interplay between electrostatic energy and translational entropy of counterions [4, 5]. The strength of the electrostatic interactions depends on the charge density along the PE which is quantified by the dimensionless Bjerrum length ℓ_B. For small charge density, counterions are dispersed away from the PE, and the chain is in an extended necklace conformation when in a good or theta-solvent [3] and is collapsed into a compact globule in a bad solvent [3, 6]. With increasing charge density, the PE attains an extended conformation, regardless of the solvent quality and counterions begin to condense onto the PE, renormalizing its charge density [3, 7, 8]. Further increase of the PE charge density results in an effective attraction between similarly-charged monomers of the PE and it collapses into a globule conformation, independent of the solvent quality [4–6, 9–12].

The compaction of a PE chain into a globular conformation is of great biological importance. For instance, biological PEs like RNA or DNA are densely packed in cells and viruses [13–15] which are orders of magnitude smaller than the contour length of the PE, requiring it to be highly compacted [16, 17]. The understanding of DNA compaction is thus crucial for future gene therapy and production of synthetic cells. Furthermore, the effective interactions driving the collapse of a single PE chain are closely connected to those resulting in aggregation of rigid PEs [18, 19]. Common biological polymers like DNA, actin and microtubules are examples of rigid PEs whose aggregates play an important role in functions like cell scaffolding making it vital to understand the nature of attractive forces between similar charges [20].

To describe the counterintuitive phenomenon of PE collapse in a good solvent, several competing theories have been proposed [4, 17, 21–25]. The first theory is based on modelling the collapsed conformation as an amorphous ionic solid [17]. For large charge density of the PE and in the presence of multivalent counterions the free energy of the solid is smaller than that of the extended PE, driving the chain collapse. This theory, however, does not predict any dependence of the gyration radius R_g on ℓ_B. In the second group of theories, it is assumed that condensed counterions and the PE monomers form dipoles [21, 23–25]. The dipoles freely rotate yielding, on average, an attractive interaction between the segments of the chain; this leads to collapse of a PE even in a good solvent. For a highly charged flexible PE in a salt-free solution, this theory predicts that the radius of gyration of the collapsed conformation scales as $R_g \sim N^{1/3} \left|\ell_B^2 - cB\right|^{-1/3}$, where B is the second virial coefficient, N is the number of chain monomers and c is a dimensional constant that depends on the details of the system [26]. This dependence is predicted for both good [21, 24, 25] and bad [21, 25] solvents. For theta-solvent with $B = 0$ [3], a simpler scaling, $R_g \sim \ell_B^{-2/3} N^{1/3}$ is obtained [21].

Finally, the third theory, referred to as counterion-fluctuation theory, argues that the collapse of a PE is due to negative pressure arising from fluctuations in the density of condensed counterions, which move freely within a PE globule [4]. Such a physical picture of the condensed counterion motion agrees with the recent results of molecular dynamics (MD) simulations [12]. The counterion-fluctuation theory, when restricted to the second virial coefficient, predicts that in a good solvent $R_g \sim \ell_B^{-1/2} N^{1/3}$. Note that all mechanisms discussed above imply a collapsed phase, $R_g \sim N^{1/3}$ for large charge density, but different dependence of R_g on ℓ_B.

Due to a great significance for applications, especially for nano-medicine and biotechnology, it is vital to have an appropriate theory of the interactions that drive the

collapse of a PE. In this Letter, we report the results of extensive MD simulations exploring the collapsed conformation of a single flexible PE chain in a good solvent. Two regimes in the dependence $R_g(\ell_B)$ have been numerically revealed: The one, consistent with the counterion fluctuation theory, $R_g \sim \ell_B^{-1/2}$ [4], and the new regime, $R_g \sim \ell_B^{-1/5}$, which we explain modifying the above theory.

MD simulations. We model a flexible PE chain as N monomers of charge e ($e > 0$ is the elementary charge) connected by harmonic springs of energy,

$$U_{bond}(r) = \frac{1}{2}k(r-a)^2, \tag{1}$$

where k is the spring constant, a is the equilibrium bond length and r is the distance between the bonded monomers. The chain and $N_c = N/Z$ neutralizing counterions, each of charge $-Ze$, with $Z = 1, 2, 3$ being the valency, are placed in a box of linear size L. Pairs of all non-bonded particles (counterions and monomers) separated by a distance r interact through the $6-12$ Lennard Jones potential cutoff at r_c:

$$U_{LJ}(r) = 4\epsilon\left[(\sigma/r)^{12} - (\sigma/r)^{6}\right]. \tag{2}$$

The values of ϵ and r_c are varied depending on the system being simulated. The electrostatic energy between charges q_i and q_j separated by r_{ij} is

$$U_c(r_{ij}) = \frac{q_i q_j}{\varepsilon r_{ij}}, \tag{3}$$

where ε is the dielectric permittivity of the solution. The charge density along the PE chain is parameterized by the dimensionless Bjerrum length ℓ_B [3]:

$$\ell_B = \frac{1}{a}\frac{e^2}{(\varepsilon k_B T)} = \frac{\beta e^2}{\varepsilon a}, \tag{4}$$

where k_B is the Boltzmann constant, T is temperature and $\beta = (k_B T)^{-1}$. Larger ℓ_B corresponds to higher charge density of the PE. In the simulations, we use $a = 1.12\sigma$, $k = 500.0\,\epsilon_0/\sigma^2$, $L = 370\,\sigma$ and the temperature, $k_B T/\epsilon_0 = 1$, is maintained through a Nosé-Hoover thermostat. The long-ranged Coulomb interactions are evaluated using the particle-particle/particle-mesh (PPPM) technique, e.g. [6, 18].

We now discuss the results from MD simulations of a single PE in a good solvent with purely repulsive LJ interactions between all non-bonded pairs of monomers and counterions. The cutoff of the LJ interaction is set at $r_c = \sigma$, and the energy constant is $\epsilon = \epsilon_0$. We simulate the system for values of ℓ_B where the equilibrium configuration of a PE is a collapsed state with $R_g \sim N^{1/3}$. The variation of the radius of gyration R_g with ℓ_B in the globular regime is shown in Fig. 1. It can be seen from Fig. 1 that for $\ell_B < \ell_B^*(Z)$ the observed dependence,

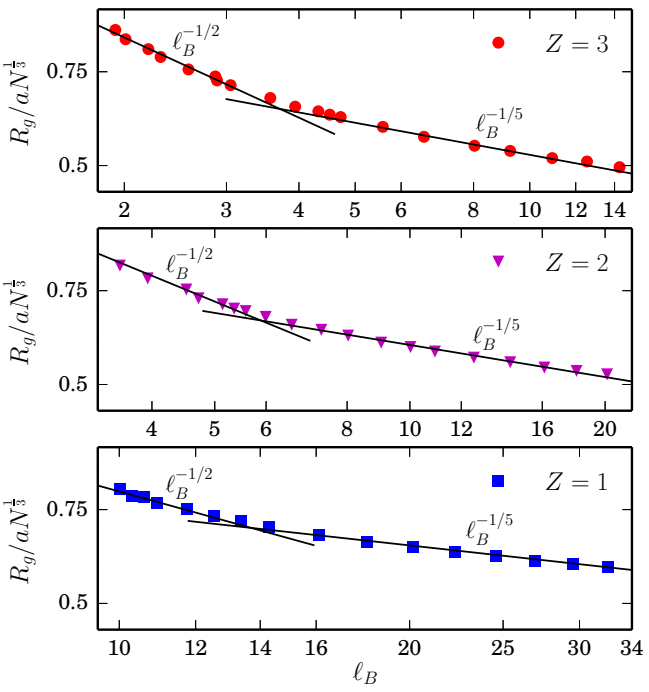

FIG. 1. Variation of the gyration radius R_g of a PE chain with the reduced Bjerrum length ℓ_B for different valencies of counterions. The chain length is $N = 204$. The two power laws intersect at $R_g/aN^{1/3} \approx 0.63$ ($Z = 3$), 0.66 ($Z = 2$) and 0.69 ($Z = 1$) with the corresponding crossover values $\ell_B^*(Z) \approx 3.71$ ($Z = 3$), 5.58 ($Z = 2$), and 13.70 ($Z = 1$).

$R_g \propto \ell_B^{-1/2} N^{1/3}$, is consistent with the predictions of the counterion-fluctuation theory [4]. For $\ell_B > \ell_B^*(Z)$, we find a crossover to a different scaling, $R_g \propto \ell_B^{-1/5} N^{1/3}$, which is not predicted by any of the existing theories. The two regimes of $\ell_B < \ell_B^*(Z)$ and $\ell_B > \ell_B^*(Z)$ will be referred to as weak and strong electrostatic regimes respectively.

Typical snapshots of the system with monovalent counterions in weak and strong electrostatic regimes are shown in Fig. 2, which demonstrates that the PE is much more compact in the strong electrostatic regime. Associated number density profile of counterions measured from the centre of mass of the collapsed PE is also shown in Fig. 2. It can be seen that the profile has a broader tail in the weak electrostatic regime, suggesting that the counterions are more loosely bound.

We have verified that the exponents and associated features seen in Fig. 1 are robust and independent on the details of the interaction by simulating two other good solvent conditions [30]: (i) LJ interactions being attractive ($r_c = 2.5\sigma$, $\epsilon = 0.25\,\epsilon_0$) for monomer-monomer pairs and purely repulsive ($r_c = 1.0\sigma$, $\epsilon = \epsilon_0$) for all other pairs and (ii) PE in the presence of explicit solvent molecules with attractive interactions between monomers and solvent ($r_c = 2.5\sigma$, $\epsilon = \epsilon_0$) and repulsive for all other pairs.

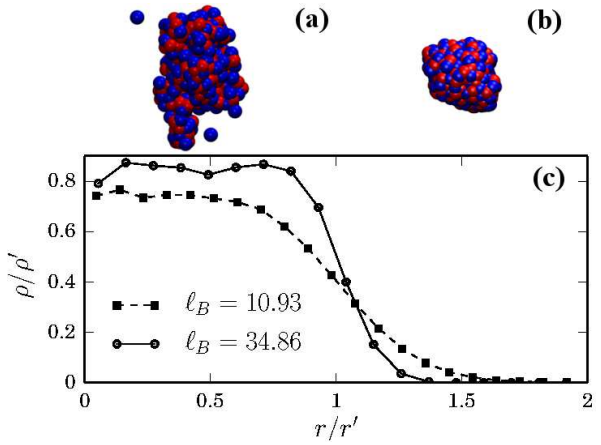

FIG. 2. Snapshots of collapsed PE in (a) weak electrostatic regime, $Z = 1$, $\ell_B = 10.93$ (left) and (b) strong electrostatic regime, $Z = 1$, $\ell_B = 34.86$ (right). (c) The corresponding radial number density profile ρ of the counterions where r is the distance of the counterion from the center of mass of the chain. r' is the distance at which the density is 50% of the density at $r = 0$ and $\rho' = N/V'$, where $V' = \frac{4}{3}\pi r'^3$.

We also confirm that the results are independent of the length of the chain for all values of ℓ_B that we have simulated (see the Supplementary Information).

The dependence of R_g on ℓ_B in the weak electrostatic regime supports the basic mechanism of the counterion-fluctuation theory as described in Ref. [4], where the PE free energy was truncated at the second virial coefficient. We now re-examine this theory to explain the dependence $R_g \propto \ell_B^{-1/5} N^{1/3}$ in the strong electrostatic regime by including more terms in the virial expansion of the PE free energy: namely, we use the simplest generalisation of the counterion-fluctuation theory [4], including the third virial coefficient C.

Theory. The free energy of the system as a function of the radius of gyration R_g of a PE chain can be written as [3, 4, 27]

$$F(R_g) = F_{\rm id.ch}(R_g) + F_{\rm vol}(R_g) + F_{\rm el}(R_g). \qquad (5)$$

Here $F_{\rm id.ch}(R_g)$ is the entropic part of the free energy corresponding to the ideal chain [3, 4, 28],

$$\beta F_{\rm id.ch} \simeq \frac{9}{4}\left(\alpha^2 + \alpha^{-2}\right), \qquad (6)$$

where $\alpha = R_g/R_{\rm g.id}$ is the expansion factor, with $R_{\rm g.id}$ being the radius of gyration of the ideal chain, $R^2_{\rm g.id} = Na^2/6$. $F_{\rm vol}$ refers to the volume interactions between the chain monomers, which may be written using the second and third virial coefficients as [3, 27]:

$$\beta F_{\rm vol} = \left(\frac{N^2 B}{2V_{\rm g}} + \frac{N^3 C}{6V_{\rm g}^2}\right) = \left(\frac{N^{1/2}\tilde{B}}{\alpha^3} + \frac{\tilde{C}}{\alpha^6}\right), \qquad (7)$$

where $V_{\rm g} = (4\pi/3)R_g^3$ is the volume of gyration and we introduce the reduced virial coefficients, $\tilde{B} = 9\sqrt{6}B/(4\pi a^3)$ and $\tilde{C} = 81C/(4\pi^2 a^6)$. Finally, $F_{\rm el}$, which takes into account all the electrostatic interactions (between the monomers and counterions) as well as the entropic part of the counterions is given by [4]:

$$\frac{\beta F_{\rm el}}{N} = \frac{3\sqrt{6}\ell_B N^{1/2}(1-\tilde{\rho})^2}{5\alpha}\left(1 - \frac{2R_g}{3R_0}\right) - \frac{3}{Z}(1-\tilde{\rho})\ln\left(\frac{R_0}{a}\right) - \frac{3}{2}\left(\frac{2}{\pi^2}\right)^{1/3}\frac{\ell_B\sqrt{6}Z^{2/3}\tilde{\rho}^{4/3}}{N^{1/6}\alpha}. \qquad (8)$$

Here $\tilde{\rho} = \rho_{\rm in}/\rho_0$ with $\rho_{\rm in}$ being the number density of counterions within the volume occupied by the polymer chain $V_{\rm g}$ and $\rho_0 = N_c/V_{\rm g} = N/(ZV_{\rm g})$ is the counterion density at the complete condensation. The value of R_0 quantifies the volume $4\pi R_0^3/3$ per chain in the solution and corresponds to L in the MD simulations. The above expression for $F_{\rm el}$ is valid for dilute solutions, $R_0 \gg R_g$ and for $N \gg 1$ [29]. The first term in the right hand side of Eq. (8) accounts (on the mean-field level) for the electrostatic interactions in the system, while the second term describes the entropic part of the counterion free energy. The third term quantifies the contribution from electrostatic correlations to the free energy, and is absent within the Poisson-Boltzmann approximation [4].

We now focus on the globular state where $R_g \sim N^{1/3}$, so that $\alpha \ll 1$. In this case, the entropic part of the free energy $F_{\rm id.ch}$ [see Eq. (6)] may be ignored when compared to the other parts of the free energy ($F_{\rm vol} + F_{\rm el}$). Also, in the collapsed regime, most of the counterions are in the vicinity of the PE, which suggests the approximation $\tilde{\rho} \approx 1$ in Eq. (8). Hence the electrostatic contribution to the free energy can be approximated as

$$\frac{\beta F_{\rm el}}{N} \approx -\frac{\tilde{Z}^2\ell_B}{N^{1/6}\alpha}, \qquad (9)$$

where $\tilde{Z}^2 = (3/2)(2/\pi^2)^{1/3}\sqrt{6}\,Z^{2/3}$. Thus for a single PE in any solvent, in the regime where the electrostatic contribution to the free energy dominates over the entropic one, Eqs. (7) and (9) yield for the free energy:

$$\frac{\beta F}{N} = -\frac{\tilde{Z}^2\ell_B}{N^{1/6}\alpha} + \frac{\tilde{B}}{N^{1/2}\alpha^3} + \frac{\tilde{C}}{N\alpha^6}. \qquad (10)$$

Note that while Eq. (10) takes into account the volume interactions between the chain monomers, such interactions with counterions may be also important for a dense globule. It is straightforward to take into account these interactions, which does not alter the form of the free energy (10), but leads to the renormalization of $\tilde{B}$ and $\tilde{C}$ (see the Supplementary Information). For simplicity we keep the same notations for the renormalized coefficients.

In what follows we consider the case of a good solvent, which corresponds to positive coefficients $\tilde{B}$ and $\tilde{C}$. To find equilibrium α and hence R_g, one needs to minimize

Eq. (10) with respect to α. The relative importance of the virial terms in Eq. (10) depends on N, the virial coefficients $\tilde{B}$ and $\tilde{C}$, and the expansion factor α. The second virial term dominates when $\alpha^3 > \tilde{C}N^{-1/2}/\tilde{B}$, which corresponds to the *weak electrostatic regime*. Neglecting the third virial term in Eq. (10) and minimizing F with respect to $\alpha = R_g/R_{\mathrm{g.id}}$, we find

$$R_g = \frac{\sqrt{\tilde{B}}aN^{1/3}}{\sqrt{2}\tilde{Z}\ell_B^{1/2}}, \tag{11}$$

as obtained in Ref. [4]. This is consistent with the MD data for $\ell_B < \ell_B^*$: $R_g \sim \ell_B^{-1/2}$, see Fig. 1.

In contrast, in the *strong electrostatic regime*, when $\alpha^3 < \tilde{C}N^{-1/2}/\tilde{B}$, the third virial term is larger than the second one. Hence, neglecting the second virial term in Eq. (10) and minimizing the free energy, we obtain

$$R_g = \frac{\tilde{C}^{1/5}aN^{1/3}}{6^{3/10}\tilde{Z}^{2/5}\ell_B^{1/5}}. \tag{12}$$

This scaling of R_g is consistent with the MD simulation data for $\ell_B > \ell_B^*$: $R_g \sim \ell_B^{-1/5}$ as shown in Fig. 1.

To check independently our approximations for the electrostatic and the volume part of the free energy, Eqs. (9) and (7), we now calculate the respective components of the internal energy and compare them to results from MD simulations. The electrostatic part of the internal energy $E_{\mathrm{el}} = \partial(\beta F_{\mathrm{el}})/\partial\beta$ is given by

$$\beta E_{\mathrm{el}}/(N\ell_B) = -\tilde{Z}^2 aN^{1/3}/\sqrt{6}R_g \sim N^{1/3}R_g^{-1}. \tag{13}$$

The scaling of E_{el} as a function of R_g is shown in Fig. 3 from the MD data, which clearly demonstrates the linear dependence of the electrostatic energy E_{el} on the inverse gyration radius R_g as obtained in Eq. (13). We note that this linear dependence is valid in both weak and strong electrostatic regimes.

Similarly, the internal energy corresponding to the volume interactions via LJ interactions, $E_{\mathrm{LJ}} = \partial(\beta F_{\mathrm{vol}})/\partial\beta$, is given by

$$\beta E_{\mathrm{LJ}}/N = NB'R_g^{-3} + N^2C'R_g^{-6}, \tag{14}$$

where $B' = (3/8\pi)\beta\partial B/\partial\beta$ and $C' = (3/32\pi^2)\beta\partial C/\partial\beta$. If the first term in the right hand side of Eq. (14) dominates, one obtains $E_{\mathrm{LJ}} \sim R_g^{-3}$; if the second one dominates, then $E_{\mathrm{LJ}} \sim R_g^{-6}$. In Fig. 4 we plot the respective internal energy due to volume interactions from our MD data. The figure convincingly illustrates the dominance of the second and third virial terms in the weak and strong electrostatic regimes correspondingly, with the crossover occuring at $R_g/aN^{1/3} \approx 0.63$ ($Z = 3$), 0.64 ($Z = 2$) and 0.68 ($Z = 1$). These values match closely with the crossover found in Fig. 1.

Conclusion. We elucidate the origin of attractive interactions in a collapsed polyelectrolyte in a good solvent using MD simulations and theoretical analysis. We

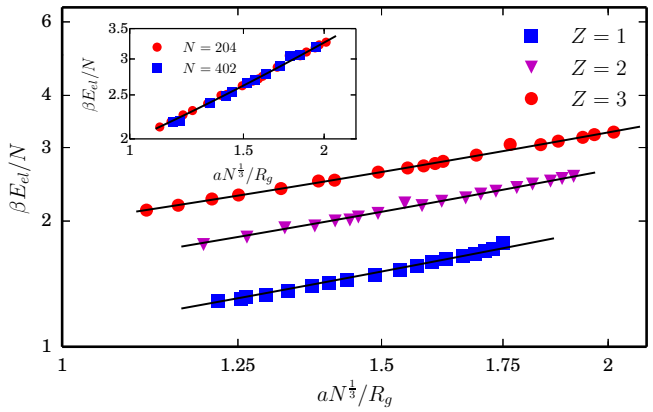

FIG. 3. Variation of the electrostatic energy E_c with the radius of gyration R_g for different valency. Inset: Variation with the chain length N.

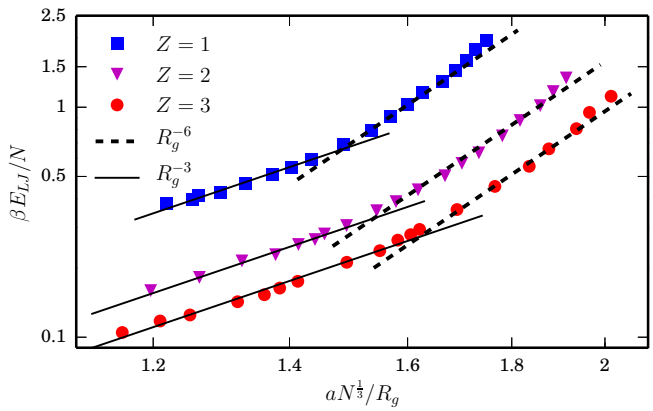

FIG. 4. Variation of the L-J energy of the system with the radius of gyration R_g for different valency.

identify two collapsed regimes, that we call as *weak* and *strong electrostatic regimes*. In the first regime the gyration radius R_g of a chain scales with Bjerrum length ℓ_B as $R_g \sim \ell_B^{-1/2}$ while in the second one as $R_g \sim \ell_B^{-1/5}$. This scaling is robust and independent on the valency of the counterions, volume interaction models between chain monomers and on the solvent models. The observed scaling in the weak electrostatic regime ($R_g \sim N^{1/3}\ell_B^{-1/2}$) is not consistent with the predictions of the theories of fluctuating dipoles ($R_g \sim N^{1/3}\ell_B^{-2/3}$) [21, 23–25], or of the amorphous ionic solid ($R_g \sim N^{1/3}\ell_B^{0}$) [17], but agrees with the counterion-fluctuation theory [4]. At the same time the scaling in the strong electrostatic regime ($R_g \sim N^{1/3}\ell_B^{-1/5}$) is not consistent with any of the existing theories.

In this Letter, we modified the counterion-fluctuation theory [4], in which density fluctuations of delocalised counterions inside a chain globule give rise to effective attractive interactions. Including the third virial term into the volume-interaction part of the free energy of

the chain $F_{\rm vol}$, we obtain the correct description for the $R_g(\ell_B)$ dependence in both weak and strong electrostatic regimes. We find that the different electrostatic regimes correspond to the dominance of different virial terms of $F_{\rm vol}$ and it may be envisaged that additional virial terms may be required at higher electrostatic strengths. We note that various theories explaining the origin of attractive interactions in a collapsed state of PE or PE gels [4, 17, 20–25, 31, 32] differ mainly in the form of the electrostatic term. As we show in our MD simulations the scaling of the electrostatic energy with the gyration radius R_g is the same for all values of ℓ_B and is consistent with the counterion-fluctuation theory. Hence, our results strongly support the counterion-fluctuation mechanism of the PE collapse in a good solvent, suggested previously in Ref. [4].

Acknowledgments: The simulations were carried out on the supercomputing machines Annapurna, Nandadevi and Satpura at the Institute of Mathematical Sciences.

* anvym@imsc.res.in
† vani@imsc.res.in
‡ rrajesh@imsc.res.in
§ nb144@leicester.ac.uk

[1] P. J. Flory, *Principles of Polymer Chemistry* (Cornell University, Ithaca, 1953).
[2] R. R. Netz and D. Andelman, Phys. Rep. **380**, 1 (2003).
[3] A. Y. Grosberg and A. R. Khokhlov, *Statistical Physics of Macromolecules* (AIP Press, Woodbury, NY, 1994).
[4] N. V. Brilliantov, D. V. Kuznetsov, and R. Klein, Phys. Rev. Lett. **81**, 1433 (1998).
[5] A. V. Dobrynin and M. Rubinstein, Prog. Poly. Science **30**, 1049 (2005).
[6] A. Varghese, S. Vemparala, and R. Rajesh, J. Chem. Phys. **135**, 154902 (2011).
[7] G. S. Manning, J. Chem. Phys. **51**, 924 (1969).
[8] A. R. Khokhlov, J. Phys. A **13**, 979 (1980).
[9] M. J. Stevens and K. Kremer, Phys. Rev. Lett. **71**, 2228 (1993).
[10] M. J. Stevens and K. Kremer, J. Chem. Phys. **103**, 1669 (1995).
[11] R. G. Winkler, M. Gold, and P. Reineker, Phys. Rev. Lett. **80**, 3731 (1998).
[12] A. A. Gavrilov, A. V. Chertovich, and E. Y. Kramarenko, Macromolecules **49**, 11031110 (2016).
[13] A. Schneemann, Ann. Rev. Microbiol. **60**, 5167 (2006).
[14] A. Siber, A. Losdorfer Bozic, and R. Podgornik, Phys. Chem. Chem. Phys. **14**, 37463765 (2012).
[15] R. F. Bruinsma, M. Comas-Garcia, R. F. Garmann, and A. Y. Grosberg, Phys. Rev. E **93**, 032405 (2016).
[16] G. C. Wong and L. Pollack, Annu. Rev. Phys. Chem. **61**, 171 (2010).
[17] F. J. Solis and O. de la Cruz, J. Chem. Phys. **112**, 2030 (2000).
[18] A. Varghese, R. Rajesh, and S. Vemparala, J. Chem. Phys. **137**, 234901 (2012).
[19] A. M. Tom, R. Rajesh, and S. Vemparala, J. Chem. Phys. **144**, 034904 (2016).
[20] Y. Levin, Rep. Prog. Phys. **65**, 1577 (2002).
[21] H. Schiessel and P. Pincus, Macromolecules **31**, 7953 (1998).
[22] R. Golestanian, M. Kardar, and T. B. Liverpool, Phys. Rev. Lett. **49**, 4456 (2016).
[23] A. Cherstvy, J. Phys. Chem. B **114**, 5241 (2010).
[24] M. Muthukumar, J. Chem. Phys. **120**, 9343 (2004).
[25] P. Kundu and A. Dua, J. Stat. Mech. , P07023 (2014).
[26] c is different in different theories of Refs. [21, 24, 25].
[27] Y. A. Budkov, A. L. Kolesnikov, and M. G. Kiselev, J. Chem. Phys. **143**, 201102 (2015).
[28] A. Y. Grosberg and D. V. Kuznetsov, Macromolecules **25**, 1970 (1992).
[29] In Ref. [4] the case of $Z = 1$ has been addressed. A straightforward generalization yields Eq. (8).
[30] See suplemental meterial.
[31] A. R. Khokhlov and E. Y. Kramarenko, Macromolecules **29**, 681 (1996).
[32] E. Y. Kramarenko, A. R. Khokhlov, and K. Yoshikawa, Macromol. Theory Simul. **9**, 249 (2000).